170 Transactions of the Korean Society of Mechanical Engineers Vol. 5, No.3, pp.170~177, 1981.

<Original>

Hydrostatic Pressure in the Center of Wire Drawing and Extrusion of Viscoplastic Material

Hung Kuk Oh*

(Received October 20, 1980)

점소성 재료의 인발과 변형역 중심에서의 정수압에 관한 연구

오 흥 국

초 록

1,200°C에서의 단조철은 점소성을 나타내며 인발과 압출시 변형 영역이 구형수렴형태가 됨을 실험을 통하여 나타난다.

이 변형역 모델로 부터 평형방정식을 사용하여 평균 압출 및 인발응력과 정수압을 계산해 낸다. 평균 압출 및 인발응력은 상계 해석 방법에 의한 결과와 비교하여 본 연구의 해석방법의 유효성을 타진하고 정수압은 다른 연구자들의 결과와 비교 검토되며 특히 냉간가공의 경우와 비교 검토된다. 그외에 마찰계수, 금형각도와 단면감소율의 영향에 대해서도 논의 된다.

Nomenclature

- r, θ, ϕ : Spherical coordinate systems
- $\overline{m}$: Friction factor
- σ_{ij} : Stress
- Ro : Entry radius of the die
- Rf : Exit radius of the die
- o : Center of the spherical coordinate system.
- τ : Tangential shear stress
- Fo, Ft : Pushing and drawing forces at the entry and exit.
- σ_0 : Effective yield stress
- r_0, r_f : Spherical radii at the entry and the exit
- σ_N : Normal pressure
- θ_0 : Half angle of the die
- p : Average pressure of σ_{rr} and $\sigma_{\theta\theta}$
- P_G : Hydrostatic pressure
- k : Tangential yield stress
- β : $\mathrm{Tan}^{-1}(\sigma_{r\theta}/\sigma_{rr})$
- A : Area
- φ : Reduction of area

* Member, Ajou University

1. Introduction

The first criterion of the chevroning in the extruded or drawn product was published by AVITZUR (Ref.1). This criterion, unhappily, had no account of the material's ductility, but took the instability, which is the material flow unbalance between the inlet and the outlet of the matrix, into consideration only. The second criterion (Ref. 2) proposed the material's ductility that is functional to the hydrostatic pressure. They had calculated the hydrostatic

pressure and the effective strain at the center of the being extruded or drawn rod. From the relation of the hydrostatic pressure to the strain at the rupture which was given by other basic experiments, the safety of the process was criticized. In order to find the hydrostatic pressure, a slab method (Ref. 3) was used by MM. L. FELGERES and P. BAQUE. Slip line method was introduced to the axisymmetric problem as this one by many researchers(Ref. 4) for ideal material. Especially MM. L. E. FARMER and PL. B. OXLEY (Ref. 5) had studied plane strain extrusion about strain hardening material in which 50% of reduction of area and 30° die angle were taken. They engraved square grids on the half plane of the specimen. After the extruding they produced the slip lines and calculated normal pressures and hydrostatic pressures on the center line. There was no singularity point in the strain-hardening case. The more strain-hardening showed the longer deformed center line and the nearer spherical deformed zone. We had prepared four cylindrical specimens divided by the middle plane on which square grids were engraved by milling and was then welded at both ends. Two specimens were for 76.6% reduction of area (Ro:31mm, Rf:15mm) and the die angle 55°, and the other two ones for 62.4% reduction of area (Ro:31mm, Rf:19mm) and the die angle 65°. They were extruded under the 400 tons press at 1200°C with the preheating 20 minutes at 650°C and then 20 minutes at 850°C. The glass powder was used as lubricant ($\overline{m}=0.10$). The used material (38C2 in French standard specification which was 0.38%C and 0.2% Cr) was the steel from which the connecting rod of automobile was forged. The ram velocities were 380mm/sec which is corresponding to $\dot{\bar{\varepsilon}}_{average}=29.5\text{sec}^{-1}$ for the 62.4% reduction of area and $\dot{\bar{\varepsilon}}_{average}=38.0\text{sec}^{-1}$ for the 76.6% reduction of area. The mechanical characteristics of the used material was $\bar{\sigma}=5.9\dot{\bar{\varepsilon}}^{0.20}(\text{kg.g/mm}^2)$ at 1200°C. The extruded half planes (Fig.1) showed a spherical deformation fields which can be explained by the influence of the variation of the effective yield stress because of material's viscosity. It is interesting to find out the hydrostatic pressure at the center of 'the spherical deformation field caused by material's viscosity. As the first step, it is assumed that the effective yield stress is averaged in the viscously deforming zone and the analysis is otherwise very difficult.

2. Analysis

We have some assumptions that the friction factor between die surface and billet is constant and the effective yield stress is the average by integration in the deformed zone. In the Fig.2, there is two zones divided. Zone 1 corresponds to a continuous spherical convergent deformation zone. Zone 2 is small normalized discontinuous field which represent all the perturbations. Starting from zone 1, equilibrium equations in spherical coordinate system;

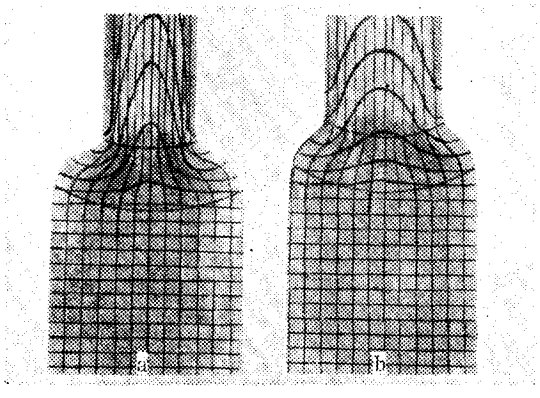

Fig. 1 Visualization of deformation zone of hot extrusion.
(a) 76.6% reduction of area, $\alpha=65°$
(b) 62.4% reduction of area, $\alpha=55°$

$$\frac{\partial \sigma_{rr}}{\partial r}+\frac{1}{r}\frac{\partial \sigma_{r\theta}}{\partial \theta}+\frac{2\sigma_{rr}-\sigma_{\phi\phi}-\sigma_{\theta\theta}+\sigma_{r\theta}\cot\theta}{r} \quad \cdots\cdots(1)$$

$$\frac{\partial \sigma_{r\theta}}{\partial r}+\frac{1}{r}\frac{\partial \sigma_{\theta\theta}}{\partial \theta}+\frac{3\sigma_{r\theta}+(\sigma_{\theta\theta}-\sigma_{\phi\phi})\cot\theta}{r} \quad \cdots\cdots(2)$$

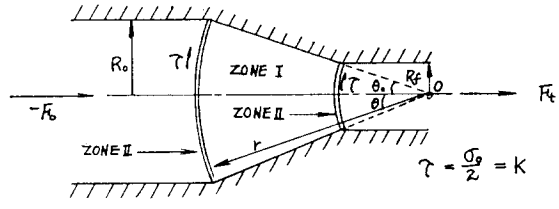

Fig. 2 Proposed spherical flow field.

In order to simplify the analysis of the model, some other assumptions;

(1) $\sigma_{r\theta}$ is dependent only upon θ,

$$\sigma_{r\theta}=\bar{m}\frac{\sigma_0}{\sqrt{3}}\frac{\sin\theta}{\sin\theta_0}$$

(2) $\sigma_{\theta\theta}=\sigma_{\phi\phi}$

(2) $2p=\sigma_{rr}+\sigma_{\theta\theta}$

(4) Take TRESCA criterion,

$\sigma_{rr}=p+k\cos\beta$, $\sigma_{\theta\theta}=p-k\cos\beta$

where $\sin\beta=\frac{\sigma_{r\theta}}{k}$ $\quad k=\frac{\sigma_0}{2}$ (see Fig. 3)

Equation (2) is reduced with the aid of the assumptions (1) and (2),

$$\frac{\partial \sigma_{\theta\theta}}{\partial \theta}+3\frac{\bar{m}}{\sqrt{3}}\sigma_0\frac{\sin\theta}{\sin\theta_0} \quad \cdots\cdots(3)$$

General solution of equation (3) is;

$$\sigma_{\theta\theta}=\frac{3}{\sqrt{3}}\bar{m}\sigma_0\frac{\cos\theta}{\sin\theta_0}+C_\theta(r) \quad \cdots\cdots(4)$$

where $C_\theta(r)$ is an integration constant.

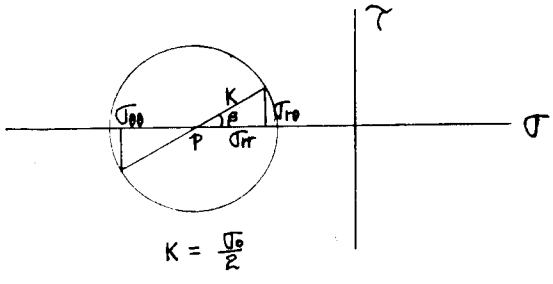

Fig. 3 MOHR circle.

We introduce equation (4) and assumption (1) into equation (1);

$$\frac{\partial \sigma_{rr}}{\partial r}+\frac{2\sigma_{rr}}{r}=\frac{1}{r}\left(2C_\theta+\frac{4\bar{m}}{\sqrt{3}}\sigma_0\frac{\cos\theta}{\sin\theta_0}\right) \quad \cdots\cdots(5)$$

And then

$$p=\sigma_{\theta\theta}+k\cos\beta$$

$$p=k\cos\beta+C_\theta(r)+\frac{3}{\sqrt{3}}\bar{m}\sigma_0\frac{\cos\theta}{\sin\theta_0}) \quad \cdots(6)$$

$$\sigma_{rr}=2k\cos\beta+C_\theta+\frac{3}{\sqrt{3}}\bar{m}\sigma_0\frac{\cos\theta}{\sin\theta_0} \quad \cdots\cdots(7)$$

Putting equation (7) into equation (5),

$$\frac{\partial C_\theta(r)}{\partial r}=\frac{1}{r}\left(-4k\cos\beta-\frac{2}{\sqrt{3}}\bar{m}\sigma_0\frac{\cos\theta}{\sin\theta_0}\right) \cdots(8)$$

It is seen here that $C_\theta(r)$ is approximately function of r only. With this assumption in equation (4), the normal pressure is well fitted with that by upper bound method. The general solution is;

$$C_\theta=\left(-4k\cos\beta-\frac{2}{\sqrt{3}}\bar{m}\sigma_0\frac{\cos\theta}{\sin\theta_0}\right)\left(\ln\frac{r}{r_0}+C\right) \quad \cdots\cdots(9)$$

The term $\cos\beta$ can be simplified;

$$\cos\beta=(1-\sin^2\beta)^{1/2}=\left(1-\frac{\sigma_{r\theta}^2}{k^2}\right)^{1/2}$$

$$=\left(1-\frac{\bar{m}\sigma_0^2}{3k^2}\frac{\sin^2\theta}{\sin^2\theta_0}\right)^{1/2}$$

$$\cos\beta\fallingdotseq 1-\frac{2}{3}\bar{m}^2\frac{\sin^2\theta}{\sin^2\theta_0} \quad \cdots\cdots(10)$$

Finally rearranging σ_{rr}

$$\sigma_{rr}=\sigma_0\left[\left\{1-2\left(\ln\frac{r}{r_0}+C\right)\right\}+\cos\theta\left\{\frac{3\bar{m}}{\sqrt{3}}\frac{1}{\sin\theta_0}-\frac{2}{\sqrt{3}}\bar{m}\frac{1}{\sin\theta_0}\left(\ln\frac{r}{r_0}+C\right)\right\}-\sin^2\theta\left\{\frac{2}{3}\bar{m}^2\frac{1}{\sin^2\theta_0}-\frac{4}{3}\bar{m}^2\frac{1}{\sin^2\theta_0}\left(\ln\frac{r}{r_0}+C\right)\right\}\right] \quad \cdots(11)$$

2.1. Drawing

We have for p,

$$p=-\frac{\sigma_0}{2}\left\{1-4\left(\ln\frac{r}{r_0}+C\right)\right\}+\sigma_0\sin^2\theta\left\{\frac{4}{3}\bar{m}^2\frac{1}{\sin^2\theta_0}\left(\ln\frac{r}{r_0}+C\right)-\frac{1}{3}\bar{m}^2\frac{1}{\sin^2\theta_0}\right\}+\sigma_0\cos\theta\left\{\frac{3}{\sqrt{3}}\bar{m}\frac{1}{\sin\theta_0}-\frac{2}{\sqrt{3}}\bar{m}\frac{1}{\sin\theta_0}\left(\ln\frac{r}{r_0}+C\right)\right\} \quad \cdots(12)$$

Through the zone Ⅱ, it is assumed that p is constant, but the material flow changes its direction only. It is given at the entry the boundary condition,

$$\int_{r=r0}p\cos dA-\int_{r=r0}\tau\sin\theta\,dA=0 \quad \cdots\cdots(13)$$

Equation (13) is resulted:

$$\int_0^{\theta_0}\left(p\sin\theta\cos\theta-\frac{\sigma_0}{2}\sin^2\theta\right)d\theta=0 \quad \cdots\cdots(14)$$

$$C=\frac{\frac{1}{4}-\frac{\bar{m}^2}{12}+\frac{\bar{m}}{\sqrt{3}}\frac{1-\cos^2\theta_0}{\sin^3\theta_0}}{1-\frac{\bar{m}^2}{3}+\frac{2}{3\sqrt{3}}\bar{m}\frac{1-\cos^3\theta_0}{\sin^3\theta_0}-\frac{1}{4}\left(\frac{\theta_0}{\sin^2\theta_0}-\cot\theta_0\right)} \quad \cdots\cdots(15)$$

where C is a integration constant.

The triaxial pressure P_G;

$$P_G=\frac{1}{3}\left(\sigma_{rr}+\sigma_{\theta\theta}+\sigma_{\phi\phi}\right)=p-\frac{k}{3}\cos\beta=p-\frac{\sigma_0}{6}\left(1-\frac{2}{3}\bar{m}^2\frac{\sin^2\theta}{\sin^2\theta_0}\right) \quad \cdots\cdots(16)$$

Therefore,

$$P_G=\sigma_0\left(\frac{1}{3}-\frac{2}{9}\bar{m}^2\frac{\sin^2\theta}{\sin^2\theta_0}\right)-\sigma_0\left(2-\frac{4}{3}\bar{m}^2\frac{\sin^2\theta}{\sin^2\theta_0}+\frac{2}{\sqrt{3}}\bar{m}\frac{\cos\theta}{\sin\theta_0}\right)\cdot\left(\ln\frac{r}{r_0}+C\right)+\frac{3}{\sqrt{3}}\bar{m}\sigma_0\frac{\cos\theta}{\sin\theta_0} \quad \cdots\cdots(17)$$

Finally the triaxial pressure at the center of the deformed billet;

$$(P_G/\sigma_0)_{\substack{r=r_f\\ \theta=0}}=\frac{1}{2}-\left(2+\frac{2}{\sqrt{3}}\bar{m}\frac{1}{\sin\theta_0}\right)\left(\ln\frac{r_f}{r_0}+C\right)+\frac{1}{\sqrt{3}}\bar{m}\frac{1}{\sin\theta_0} \quad \cdots(18)$$

For the purpose of judgement of the validity of this method of analysis, calculations of normal pressure make it possible to compare with the results of AVITZUR (Ref. 6). In the Fig. 2,

$$Ft=\int_{r=r_f}\left(p_{r=r_f}\cos\theta\,dA+\tau\sin\theta\,dA\right) \cdots(19)$$

where Ft is the drawing force. The normal drawing force;

$$\frac{\sigma_N}{\sigma_0}=\frac{Ft}{\pi R_f^2\sigma_0}=\frac{1}{2}\left\{1-4\left(\ln\frac{r_f}{r_0}+C\right)\right\}+\frac{1}{2}\left\{\frac{4}{3}\bar{m}^2\left(\ln\frac{r_f}{r_0}+C\right)-\frac{1}{3}\bar{m}^2\right\}+\frac{2}{\sin^3\theta_0}\left(\frac{1}{3}-\frac{\cos^3\theta_0}{3}\right)\cdot\left\{\frac{3}{\sqrt{3}}\bar{m}-\frac{2}{\sqrt{3}}\bar{m}\left(\ln\frac{r_f}{r_0}+C\right)\right\}+\frac{1}{2}\left(\frac{\theta_0}{\sin^2\theta_0}-\cot\theta_0\right) \quad \cdots\cdots(20)$$

2.2. Extrusion

Boundary conditions are only different from the case of drawing.

$$p=\frac{\sigma_0}{2}\left\{1-4\left(\ln\frac{r}{r_f}+C\right)\right\}+\sigma_0\sin^2\theta\left\{\frac{4}{3}\bar{m}^2\frac{1}{\sin^2\theta_0}\left(\ln\frac{r}{r_f}+C\right)-\frac{1}{3}\bar{m}^2\frac{1}{\sin^2\theta_0}\right\}+\sigma_0\cos\theta\left\{\frac{3}{\sqrt{3}}\bar{m}\frac{1}{\sin\theta_0}-\frac{2}{\sqrt{3}}\bar{m}\frac{1}{\sin\theta_0}\left(\ln\frac{r}{r_f}+C\right)\right\} \quad \cdots\cdots(21)$$

$$Ft=\int_{\theta=0}^{\theta_0}\left(p_{r=r_f}\cos\theta\,dA+\tau\sin\theta\,dA\right)=0 \quad \cdots\cdots(22)$$

From equation (22)

$$C=\frac{\frac{1}{4}-\frac{\bar{m}^2}{12}+\frac{\bar{m}}{\sqrt{3}}\frac{1-\cos^3\theta_0}{\sin^3\varepsilon_0}}{1-\frac{\bar{m}^2}{3}+\frac{2}{3\sqrt{3}}\bar{m}\frac{1-\cos^3\theta_0}{\sin^3\theta_0}+\frac{1}{4}\left(\frac{\theta_0}{\sin^2\theta_0}-\cot\theta_0\right)} \quad \cdots\cdots(23)$$

Finally

$$(P_G/\sigma_0)_{\substack{r=r_f\\ \theta=0}}=\frac{1}{2}-\left(2+\frac{2}{\sqrt{3}}\overline{m}\frac{1}{\sin\theta_0}\right)C+\frac{3}{\sqrt{3}}\overline{m}\frac{1}{\sin\theta_0} \quad \cdots\cdots(24)$$

For the purpose of judgement of the validity of this method of analysis, calculations of normal pressure make it possible to compare with the results of AVITZUR (Ref. 6).

$$Fo=\int_A(p_{r=r_0}\cos\theta\,dA-\tau dA\sin\theta)$$

$$\frac{\sigma_N}{\sigma_0}=\frac{1}{2}\left\{1-4\left(\ln\frac{r_0}{r_f}+C\right)\right\}+\frac{1}{2}\left\{\frac{4}{3}\overline{m}^2\left(\ln\frac{r_0}{r_f}+C\right)-\frac{\overline{m}^2}{3}\right\}+\frac{2}{\sin^3\theta_0}\left(\frac{1}{3}-\frac{\cos^3\theta_0}{3}\right)\cdot\left\{\frac{3}{\sqrt{3}}\overline{m}-\frac{2}{\sqrt{3}}\overline{m}\left(\ln\frac{r_0}{r_f}+C\right)\right\}-\frac{1}{2}\left(\frac{\theta_0}{\sin^2\theta_0}-\cot\theta_0\right) \quad \cdots\cdots(25)$$

3. Analytic Results

3.1. Drawing

We can see in Table 1 the influence of θ_0 and the influence of φ about the normal pressure and the hydrostatic pressure where $\overline{m}=0.03$. It also can be seen in Table 2 that, when θ_0 increases, the normal pressure and the hydrostatic pressure are increased at $\overline{m}=0.10$ and $\varphi=0.10$. Table 3 shows that, when $\overline{m}$ increases, both of two are increased at $\varphi=0.30$ and $\theta_0=20°$. It is also showed in Table 4 that, when φ increases, both of two are increased at $\overline{m}=0.10$ and $\theta_0=15°$. The normal pressure is little smaller than that of AVITZUR. Probably it comes from the method of analysis by upper bound. (Fig. 4), (Ref. 5). The hydrostatic pressure is compared with the results of M. MOHAMDEIN based on the slip line method in the case of cold drawing ($\overline{m}=0$), (Fig. 5), (Ref. 3). The former increases with the reduction of area but the latter decreases. Both of two increase with the die angle.

Table 1 Normal pressures and hydrostatic pressures at several conditions of work($\overline{m}=0.03$).

$\overline{m}$	φ	θ_0	σ_N/σ_0	$(P_G/\sigma_0)_{\substack{r=r_f\\ \theta=0}}$
0.03	0.10	5	0.1845	0.1561
0.03	0.10	10	0.2326	0.1760
0.03	0.10	15	0.2844	0.2032
0.03	0.10	20	0.3471	0.2327
0.03	0.10	25	0.4079	0.2637
0.03	0.10	30	0.4711	0.2961
0.03	0.10	35	0.5369	0.3299
0.03	0.10	40	0.6058	0.3653
0.03	0.20	5	0.3256	0.2973
0.03	0.20	10	0.3620	0.3055
0.03	0.20	15	0.4139	0.3289
0.03	0.20	20	0.4706	0.3565
0.03	0.30	5	0.4856	0.4574
0.03	0.30	10	0.5087	0.4524
0.03	0.30	15	0.5562	0.4713
0.03	0.30	20	0.6106	0.4968
0.03	0.40	5	0.6702	0.6421
0.03	0.40	10	0.6781	0.6219
0.03	0.40	15	0.7204	0.6358
0.03	0.40	20	0.7723	0.6587
0.03	0.50	5	0.8887	0.8606
0.03	0.50	10	0.8784	0.8220
0.03	0.50	15	0.9147	0.8303
0.03	0.50	20	0.9636	0.8503

Table 2 Influences of the die angle.

$\overline{m}$	φ	θ_0	σ_N/σ_0	$(P_G/\sigma_0)_{\substack{r=r_f\\ \theta=0}}$
0.10	0.10	10	0.2566	0.2017
0.10	0.10	15	0.3043	0.2237
0.10	0.10	20	0.3588	0.2519
0.10	0.10	25	0.4172	0.2832
0.10	0.10	30	0.4787	0.3167
0.10	0.10	35	0.5433	0.3521
0.10	0.10	40	0.6113	0.3895

Table 3 Influences of the friction factor.

$\overline{m}$	φ	θ_0	σ_N/σ_0	$(P_G/\sigma_0)_{\substack{r=r_f\\ \theta=0}}$
0.00	0.30	20	0.5932	0.4750
0.05	0.30	20	0.6221	0.5111
0.10	0.30	20	0.6505	0.5457

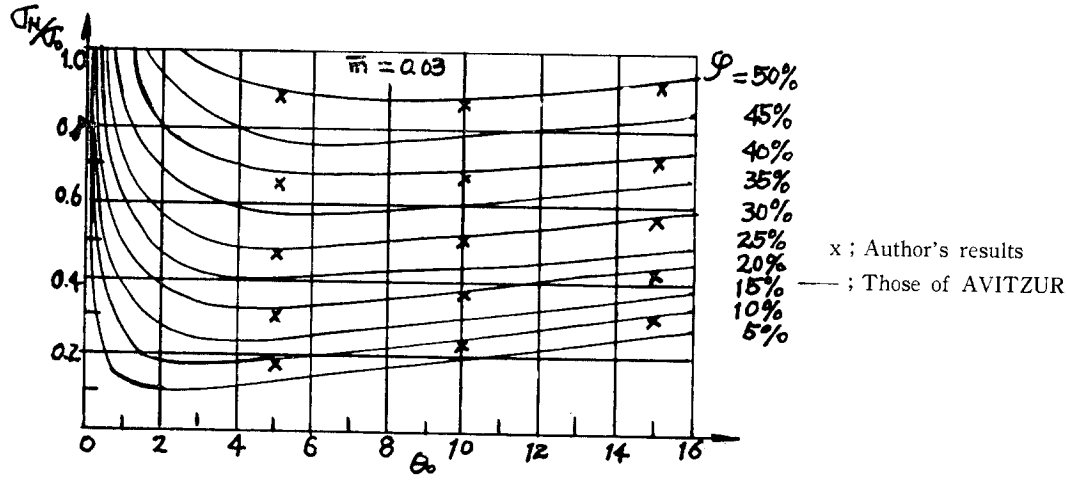

Fig. 4 Comparison between author's normal pressures and those of AVITZUR (Ref. 5).

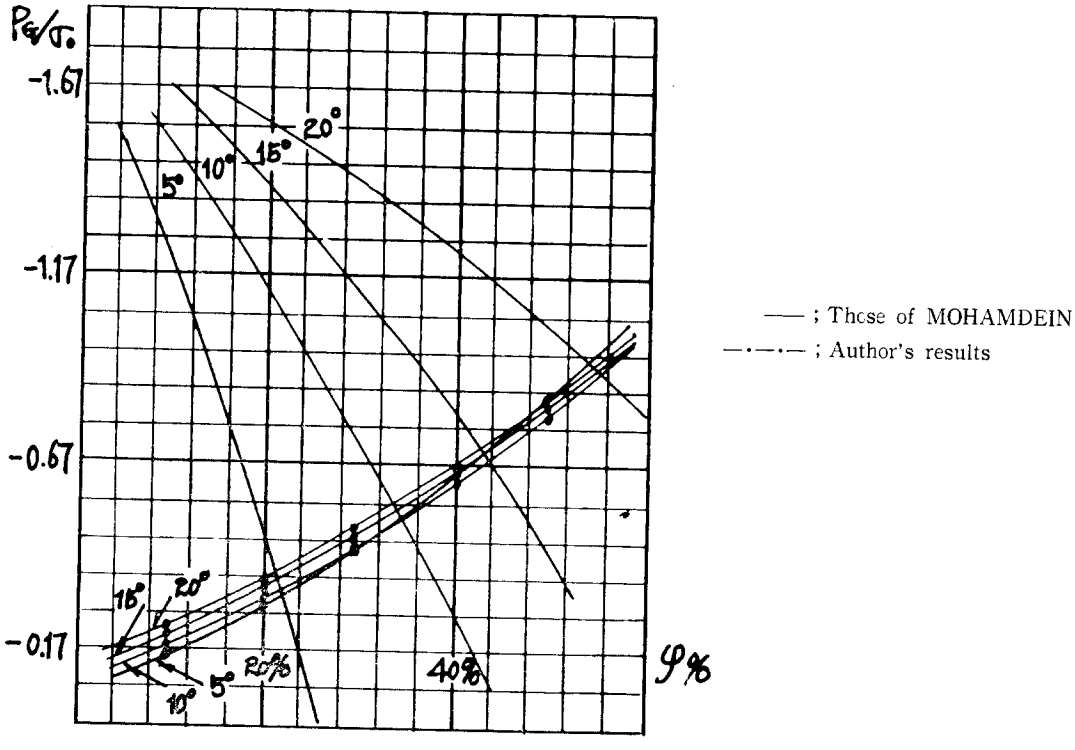

Fig. 5 Comparison between Author's normal pressures and those of M. MOHAMDEIN.

0.15	0.30	20	0.6782	0.5781
0.20	0.30	20	0.7053	0.6081
0.30	0.30	20	0.7578	0.6591
0.50	0.30	20	0.8556	0.7184

Table 4 Influences of the reductionof area.

$\overline{m}$	φ	θ_0	σ_N/σ_0	$(P_G/\sigma_0)_{\substack{r=r_f \\ \theta=0}}$
0.10	0.10	15	0.304	0.2237
0.10	0.15	15	0.3738	0.2936
0.10	0.20	15	0.4475	0.3677
0.10	0.25	15	0.5260	0.4469
0.10	0.30	15	0.6098	0.5311
0.10	0.35	15	0.7000	0.6217
0.10	0.40	15	0.7973	0.7196
0.10	0.45	15	0.9031	0.8260

3.2. Extrusion

Table 5 shows the influences of friction factor, reduction of area and die angle about the normal pressure and hydrostatic pressure. The increase of θ_0 makes the hydrostatic pressure more depressive, the greater friction factor the more compressive and the reduction of area changes not the hydrostatic pressure. The influences about normal pressure is like the ideal material case. The normal pressure is compared in Fig. 6 with that of AVITZUR particularly at $\overline{m}=0.10$ and $\varphi=0.50$. The former is 6% smaller than the latter. It also comes, I think, from the upper bound method of AVITZUR. The hydrostatic pressure is compared in Fig. 7 with that of M. FELGERES and that by slip line method in cold extrusion when $\overline{m}=0$. The hydrostatic pressure in cold extrusion by slip line method is very depressive with respect to that of hot viscoplastic material's extrusion. That of M. FELGERES is little different from author's result because, I think, his flowfield is spherical.

Hot drawing and extrusion have furnished

Table 5 Normal pressure and hydrostatic pressure in extrusion.

$\overline{m}$	φ	θ_0	σ_N/σ_0	$(P_G/\sigma_0)_{\substack{r=r_f \\ \theta=0}}$
0.00	0.50	40	−1.1910	−0.2490
0.00	0.50	50	−1.3411	−0.3240
0.00	0.50	60	−1.5121	−0.4095
0.00	0.50	70	−1.7128	−0.5098
0.10	0.50	40	−1.2441	−0.2294
0.10	0.50	50	−1.3824	−0.3000
0.10	0.50	55	−1.4606	−0.3392
0.10	0.50	60	−1.5457	−0.3818
0.10	0.50	65	−1.6388	−0.4283
0.10	0.50	70	−1.7413	−0.4796
0.10	0.75	40	−1.9902	−0.2294
0.10	0.75	50	−2.1168	−0.3000
0.10	0.75	55	−2.1908	−0.3392
0.10	0.75	60	−2.2725	−0.3818
0.10	0.75	65	−2.3628	−0.4283
0.10	0.75	70	−2.4639	−0.4796
0.20	0.50	40	−1.2924	−0.2176
0.20	0.50	50	−1.4191	−0.2836
0.20	0.50	55	−1.4930	−0.3208
0.20	0.50	60	−1.5747	−0.3617
0.20	0.50	65	−1.6650	−0.4070
0.20	0.50	70	−1.7652	−0.4574
0.20	0.75	40	−2.0869	−0.2176
0.20	0.75	50	−2.1902	−0.2836
0.20	0.75	55	−2.2567	−0.3208
0.20	0.75	60	−2.3305	−0.3617
0.20	0.75	65	−2.4152	−0.4070
0.20	0.75	70	−2.5109	−0.4574
0.20	0.40	60	−1.3759	−0.3617
0.20	0.50	60	−1.5747	−0.3617
0.20	0.60	60	−1.8180	−0.3617
0.20	0.70	60	−2.1817	−0.3617
0.20	0.80	60	−2.5738	−0.3617
0.20	0.90	60	−3.3296	−0.3617
0.00	0.75	60	−2.2052	−0.4095
0.05	0.75	60	−2.2400	−0.3948
0.10	0.75	60	−2.2725	−0.3818
0.15	0.75	60	−2.3026	−0.3707
0.20	0.75	60	−2.3305	−0.3617
0.30	0.75	60	−2.3793	−0.3511
0.40	0.75	60	−2.4188	−0.3518
0.50	0.75	60	−2.4491	−0.3658
0.70	0.75	60	−2.4823	0−0.443
0.60	0.50	40	−1.4397	−0.2901

0.60	0.50	50	−1.5195	−0.3392
0.60	0.50	60	−1.6455	−0.3954
0.60	0.50	70	−1.8148	−0.4835
0.80	0.80	40	−2.7912	−0.4283
0.80	0.80	50	−2.7237	−0.4584
0.80	0.80	60	−2.7526	−0.5127
0.80	0.80	70	−2.8591	−0.5988
0.80	0.90	40	−3.7788	−0.4283
0.80	0.90	50	−3.6177	−0.4584
0.80	0.90	60	−3.5854	−0.5127
0.80	0.90	70	−3.6513	−0.5988

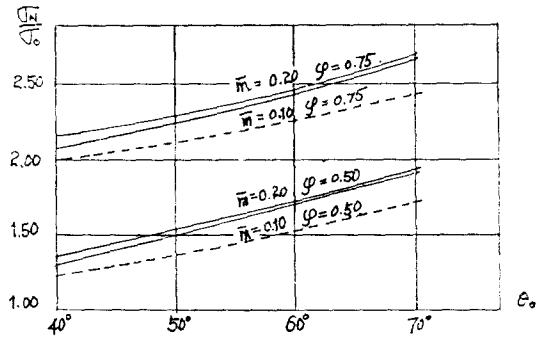

Fig. 6 Comparison between AVITZUR'S normal pressure and author's results.
———By AVITZUR
.....Author's results.

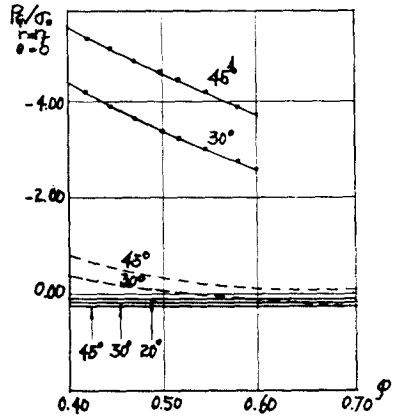

Fig. 7 Comparison of author's results of hydrostatic pressure at center line in extrusion with that of M. FELGERE and that by slip ine method ($\bar{m}$=0.00).
———By M.FELGERE
—·—·—By slip line method
.....Author's resultss

spherical flow-field from the experiments at 1200°C because of the material's viscosity. The normal pressure by this flow field is little different by author's method from that by upper bound one. The hydrostatic pressure becomes more depressive with the greater friction factor, die angle and reduction of area in hot viscoplastic material's drawing, while in cold drawing the reduction of area has reverse effect (Fig. 5). The hydrostatic pressure in hot viscoplastic material's extrusion is more depressive with the greater die angle, but it is more compressive with the greater friction facor. Surprisingly it varies not with the reduction of area. It is noted conclusively hat the material's viscosity gives many interesting unusual results in comparison with the ideal material.

References

1. Avitzur B.-Analysis of central bursting defects in extrusion and wire drawing-Trans A.S.M.E.-J. of eng. for ind. (1968) 90 p. 79
2. Thomason D.F. (1969~1970)-"A theoretical estimate of the limits of ductility in the free extrusion process"-Proc. inst. mech. engrs-Vol. 184 N47-p. 896
3. Felgeres L., Baque P.-"Contributions à l'étude du défaut en chevron-Avril 1975-Rapport N°1-Contrat R.N.U.R./ARMINES
4. Mohamdein-Thése doc. ing.-Juin 1977-p. 29~62, Paris VI.
5. Farmer L. E., Oxley P.L.B.-A slip line field for plane strain extrusion of a strainhardening material-J. Mech. Phys. Solids (1971) 19 p. 369
6. Betzalei Avitzur-Metal Forming-Process and Analysis-Mc Graw Hill p. 153~217
7. Zimmerman Z., Avitzu R B.- Analysis of the effect of strain-hardening on central bursting defects in drawing and extrusion-Trans. A.S.M. E.-J. of eng. for ind. (1970) 92 p. 135
8. Avitzur B.-New improved criterion for the prevention of central burst in wire drawing and extrusion-Wire Journal (Nov. 1974) p. 77